Which spectral lines trace what physical processes in the Galactic Center? First results: line list and LTE modeling

Alyssa Bulatek (she/her)[1], Adam Ginsburg[1], Katharina Immer[2], Desmond Jeff[1], Christian Henkel[3,4,5], Karl M. Menten[3], Jeremy Darling[6]

1. University of Florida, 2. University of Leiden, 3. Max-Planck-Institut für Radioastronomie, 4. King Abdulaziz University, 5. Xinjiang Astronomical Observatory, 6. Center for Astrophysics and Space Astronomy, CU Boulder

Motivation

In the disk of the Milky Way, certain molecules are used as "rule of thumb" tracers for processes in the interstellar medium. Some example processes/tracers include:

- *Outflows from protostars:* high-velocity isotopologues of CO (carbon monoxide)
- *Hot star-forming cores:* CH_3OH (methanol), CH_3CN (methyl cyanide)
- *Low-velocity shocks:* SiO (silicon monoxide), HNCO (isocyanic acid)
- *Dense gas:* HCN (hydrogen cyanide), HCO+ (formyl cation)

In extreme environments like the centers of galaxies, these tracers fail. SiO is observed in all clouds in the Milky Way's Central Molecular Zone (CMZ) so it cannot serve as a unique outflow tracer like it can in the Galactic disk. The CMZ is very dense (10^4 to 10^7 cm^{-3}), so traditional dense gas tracers aren't useful to trace the densest parts of the ISM. The same is true for tracers of hot cores and shocks; their emission is widespread throughout the CMZ. **We need unique tracers for star formation processes that can be used in CMZs and starburst galaxies.**

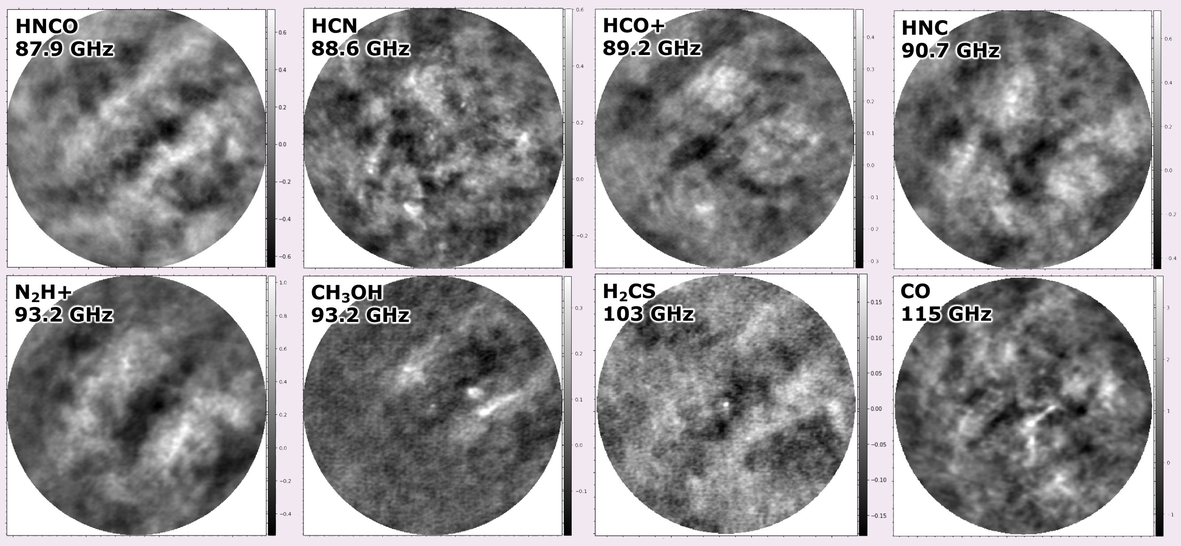

Figure 1. Integrated intensity maps (in units of Jy beam^{-1} km s^{-1}) of molecules near the water maser in The Brick. Though there are a few molecules that have some coherence, many molecules reveal the complicated underlying structure of the CMZ: multiple layers of turbulent material.

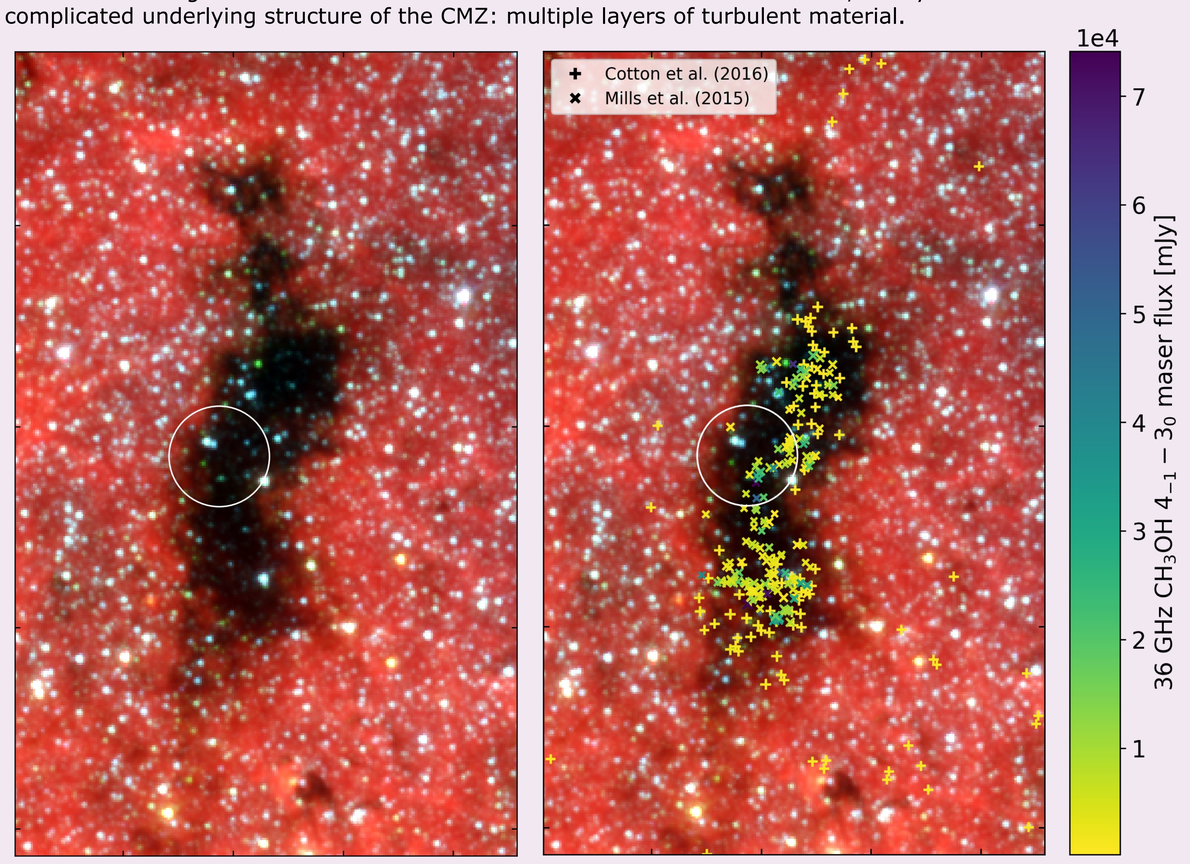

Figure 2. *Left:* three-color image of The Brick from *Spitzer* IRAC data (RGB = 8 μm, 4.5 μm, 3.6 μm). The circle shows our pointing and has a radius of 30". *Right:* same as left. +'s and x's are locations of 36 GHz class I methanol masers from Table 2 in Cotton et al. (2016) and Table 4 in Mills et al. (2015) respectively.

The Survey

Telescope	Atacama Large Millimeter/submillimeter Array (ALMA) 12-m
Pointing	"maser core" in The Brick, same as Walker et al. (2021)
Frequency coverage	Bands 3, 4, and part of 6
Angular resolution	1.72" by 1.40" (about 0.07 pc)

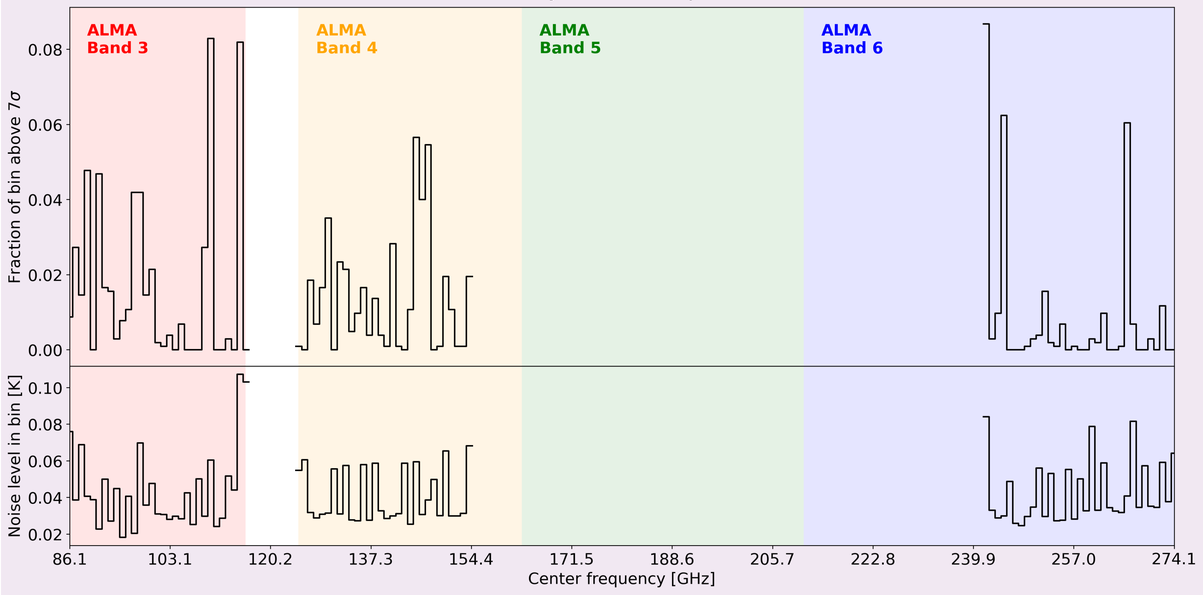

Figure 3. Density of spectral lines in a 1 GHz-binned representation of the delivered survey data. This density was calculated from peak intensity spectra, which trace localized emission (in many frames, this is the central maser source). The field-of-view across all spectral windows was limited to 0.8 times the primary beam size of the highest-frequency spectral window in our data, at the top of Band 6.

LTE Modeling

Temperature/column density estimates from fitting CH_3CN ladders → Assuming the same values for all molecules, produce **full LTE model**

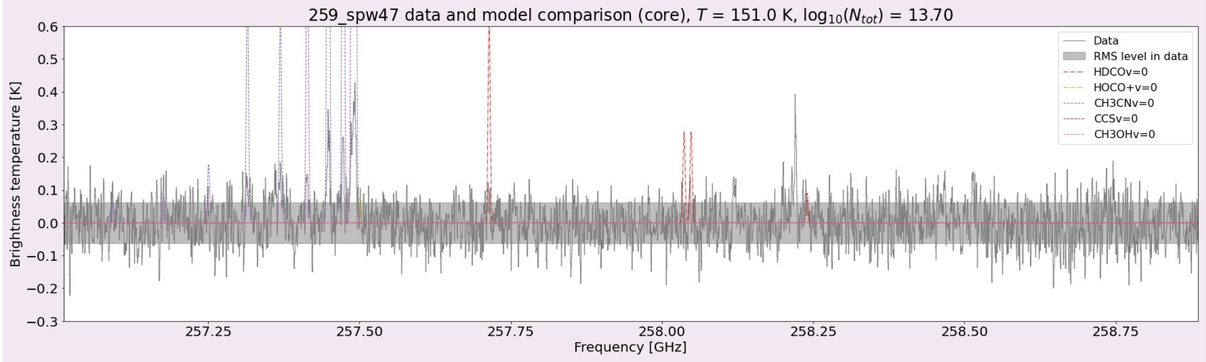

Figure 4. Comparison of data (solid grey) and model (non-solid, colorful) spectra generated with XCLASS in the maser core. Each molecule is modeled separately with XCLASS. The CH_3CN J = 14 ladder shows up in the spectrum for the maser core. The temperature and column density used to generate the models are very close to the estimates we gleaned from our initial CH_3CN fitting, but these values likely do not apply to all transitions of all molecules. This is why the strength of the model lines does not match the data.

Detection of Methanol "Dasar" Transition at 107 GHz

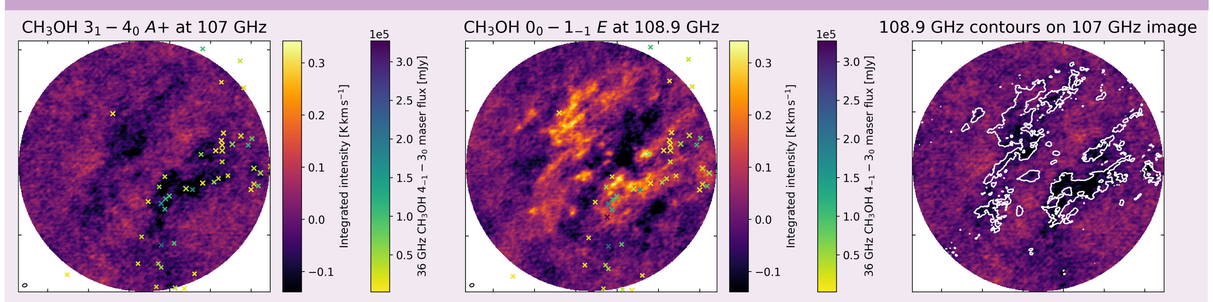

Figure 5. Comparison of 107 GHz methanol transition with nearby 108.9 GHz transition. All images are integrated intensity maps. Right panel shows the integrated intensity map of 107 GHz transition with contours of 108.9 GHz transition overplotted. Note spatial correspondence between absorption in the 107 GHz line with emission in the 108.9 GHz line. x's are 36 GHz methanol masers from Mills et al. (2015).

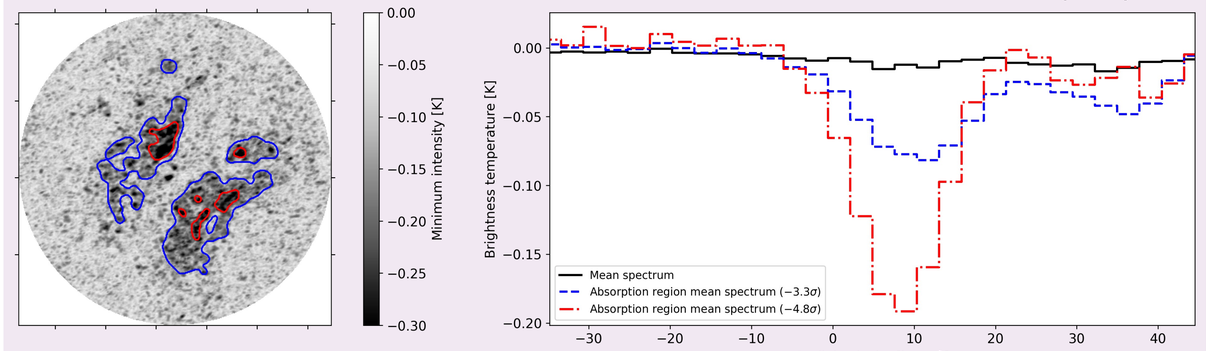

Figure 6. Spectral extraction of regions within the area where absorption is occurring. *Left:* minimum intensity map of 107 GHz transition. *Right:* spectra extracted from different regions in map: black solid line is across whole map, blue dotted line is across −3.3σ region, red dot-dashed line is across −4.8σ region.

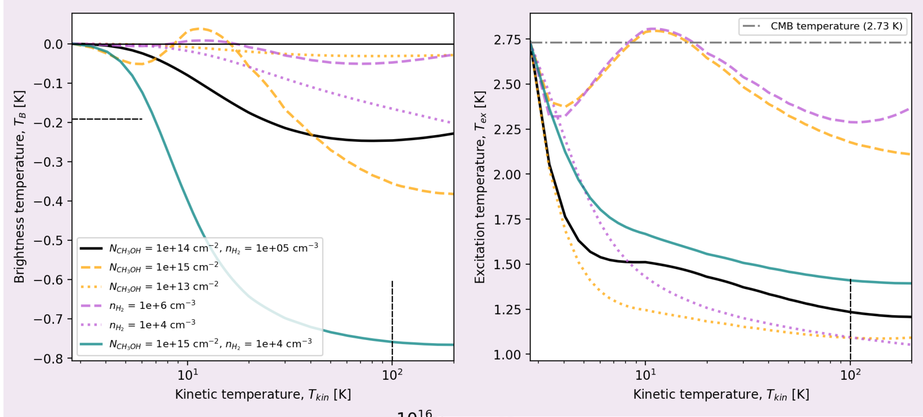

Figure 7. Behavior of the 107 GHz transition (T_B and T_{ex}) as a function of T_{kin} for several combinations of column and volume density. Modeled with pyRADEX. There are broad ranges over which dasing occurs, but also stretches where it stops (e.g., at higher column and volume densities, from T_{kin} ~ 10 and 20 K).

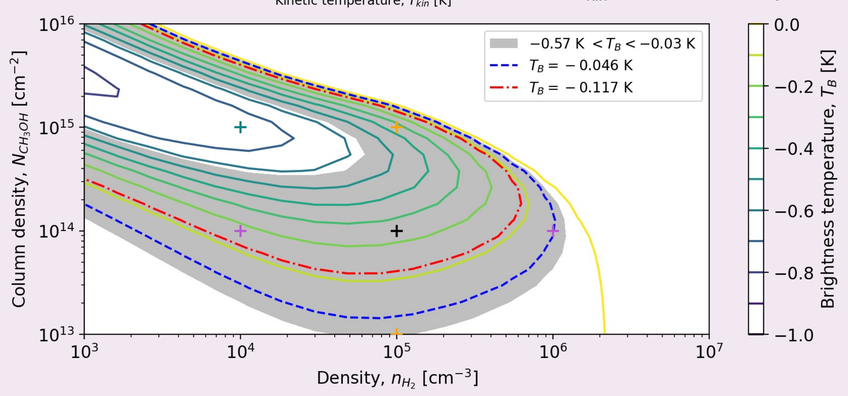

Figure 8. Exploration of the behavior of the 107 GHz transition as a function of column density $N(CH_3OH)$ and density $n(H_2)$. Modeled using pyRADEX with a kinetic temperature of T_{kin} = 100 K. The shaded region shows where we observe dasing. The red and blue lines show the minimum values from the extracted spectra in Figure 6. Crosses mark the parameter space explored in Figure 7.

JWST 2221

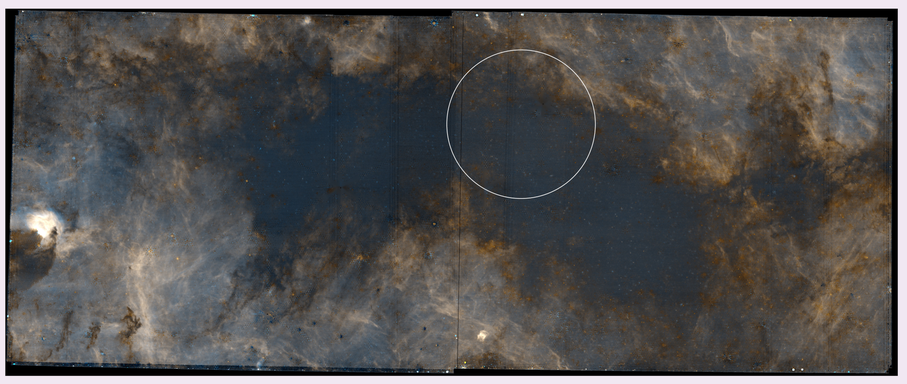

Figure 9. View of The Brick through the NIRCAM instrument on *JWST*. The circle marks the pointing of the line survey (radius 30"). Blue is mostly the F466N filter; brown is mostly the F405N filter. Our *JWST* project will count and classify YSOs embedded in The Brick using both NIRCAM and MIRI data.

References

Arce et al. 2010, ApJ, 715, 1170.
Battersby et al. 2011, A&A, 535, A128.
Churchwell et al. 2009, PASP, 121, 213.
Cotton et al. 2016, ApJS, 227, 10.
Darling et al. 2012, ApJL, 749, L33.
Ginsburg et al. 2016, A&A, 586, A50.
Jones et al. 2012, MNRAS, 419, 2961.
Kauffmann et al. 2017, A&A, 603, A89.
Leurini et al. 2016, A&A, 592, A31.
Lu et al. 2021, ApJ, 909, 177.
Mills et al. 2015, ApJ, 805, 72.
Molinari et al. 2016, A&A, 591, A149.
Morris et al. 1996, ARA&A, 34, 645.
Rathborne et al. 2014, ApJ, 786, 140.
Walker et al. 2021, MNRAS, 503, 77.

Email: abulatek@ufl.edu **Website:** abulatek.github.io